Accepted manuscript – postprint version
Hok, L., Ulm, L., Tandarić, T., Krivohlavek, A., Šakić, D., & Vrček, V. (2018). Chlorination of 5-fluorouracil: Reaction mechanism and ecotoxicity assessment of chlorinated products. *Chemosphere*, *207*, 612–619. https://doi.org/10.1016/j.chemosphere.2018.05.140

Chlorination of 5-Fluorouracil: Reaction Mechanism and Ecotoxicity Assessment of Chlorinated Products

Lucija Hok,[1] Lea Ulm,[2] Tana Tandarić,[3] Adela Krivohlavek,[2] Davor Šakić,[1] and Valerije Vrček[1,*]

[1] Faculty of Pharmacy and Biochemistry, University of Zagreb, Ante Kovačića 1, Zagreb, Croatia

[2] Andrija Štampar Teaching Institute of Public Health, Mirogojska 16, Zagreb, Croatia

[3] Division of Organic Chemistry and Biochemistry, Ruđer Bošković Institute, Bijenička 54, Zagreb, Croatia

*Corresponding author: Prof. dr. Valerije Vrček
Faculty of Pharmacy and Biochemistry, University of Zagreb, A. Kovačića 1, Zagreb, Croatia
E-mail: vvrcek@pharma.hr
Tel: +385-1-6394441

Abstract

What happens to drugs in the chlorinating environment? Degradation products may vary in pharmacological profiles and in ecotoxicity potentials compared to the parent compound. This study combines synthesis, NMR spectroscopy, quantum chemical calculations, and toxicity experiments on *Daphnia magna* to investigate chemical fate of antineoplastic drug 5-fluorouracil (5-FU) in chlorinated environment, which is common in waste-water treatment procedures, but also endogenous in activated neutrophils. A reduction of toxicity (EC_{50} after 48 hours is 50% higher than for the parent 5-FU) was observed after the first chlorination step, in which a chlorohydrin 5-chloro-5-fluoro-6-hydroxy-5,6-dihydrouracil was formed. Further chlorination leads to N-chlorinated intermediate, that undergoes the pyrimidine ring opening reaction. The final product, 2-chloro-2-fluoro-3,3-dihydroxypropanoic acid was obtained after the loss of the chlorinated urea fragment. This is the most potent compound in the reaction sequence, with toxicity parameter EC_{50}, after 48 hours, more than twice lower compared to the parent 5-FU. Clearly, the contact time between chlorinating species and degradation products provide different ecotoxicological properties of reaction mixtures. Interplay between experimental and theoretical procedures, to properly describe reaction pathways and provide more information on toxicity profiles, is a way forward in environmental science research.

Keywords

5-fluorouracil, hypochlorous acid, ecotoxicity, reaction mechanism, DFT calculation

1. Introduction

5-Fluorouracil (5-FU) is a pyrimidine antimetabolite introduced in the clinic as an anticancer drug (Jordan, 2016). It is one of the most widely prescribed cytostatic pharmaceutical for the last 60 years. Up to 30% of its administered dose is excreted as the parent form that enters the environment (Kosjek and Heath, 2011). The measured environmental concentrations of 5-FU range from 5 – 100 ng/L in wastewater treatment plant influents (Kosjek et al., 2013), and may amount to more than 100 μg/L in hospital wastewaters (Mahnik et al., 2004). 5-FU is relatively stable in water, but undergoes different transformation reactions induced by chemical water treatments, such as ozonolysis or chlorination. The latter is the most widely used method for chemical treatment and disinfection of water (USEPA, 2004). Since 5-FU has been identified in wastewaters and surface waters (Mahnik et al., 2007) the potential exists for the formation of its disinfection byproducts during water chlorination.

The reaction between 5-FU and hypochlorous acid (HOCl) is the fundamental process which can occur in activated neutrophils in cancer patients (Winterbourn et al., 2016) or during chemical treatment of (hospital) wastewaters (Deborde and Gunten, 2008; Acero et al., 2010). Therefore, the chlorination of 5-FU is of utmost importance in medicinal and environmental chemistry. The elementary chemical reaction, the one with no enzyme assistance, is simple yet so intricate process. Mechanistic details underlying a HOCl-induced transformation of 5-FU have not been resolved. In addition, chlorinated products are unknown or only tentatively assigned, and their environmental effects have not been investigated. For this reason the chemical fate of 5-FU under chlorination conditions should be revisited.

We set to investigate the chlorination mechanism which gives rise to stable products. By using NMR spectroscopy coupled to high-level computational techniques, the relevant

reaction profiles were described in details. The chlorinated products were isolated and their ecotoxicological effects were studied in acute immobilization assays with crustacean *Daphnia magna*.

In this work the interplay between experimental and theoretical methods has been shown as an efficient approach in solving some environmental problems. The results on the chlorination of 5-FU are relevant for a series of pyrimidines, and for nucleobase derivatives in particular.

2. Material and Methods

2.1. General procedures and equipments

The syntheses were carried out in distilled water, and kinetic experiments in the phosphate buffer. Melting point was determined with a Büchi apparatus. For HPLC-MS analysis, ultra high-speed single quadropole mass spectrometer with ultra high-speed liquid chromatography, Prominence UFLC+LCMS-2020 from Shimadzu Corp. (Kyoto, Japan) was used. Separation was performed on a Zorbax SB C18 (150x2.1mm 3.5µm; Agilent Technologies Deutschland GmbH, Waldbronn, Germany) narrow bore LC column with 0.1% formic acid in water/ 0.1% formic acid in methanol as isocratic mobile phase in ratio (10/90) with flow-rate of 0.2 mL min^{-2}. MS scanning in the range m/z 50-350 for negative and positive electrospray ionisation was used (mass spectra recorded in positive ion mode in SI). The interface parameters were: temperature of electrospray probe (ESI) = 350 °C, curved desolvation line (CDL) temperature or temperature of the heated capillary = 250 °C, the nebulizing and drying gas was N_2 with flow-rate 1.5 L min^{-2}, 15 L min^{-2} , respectively, and the block temperature was set at 200 °C. The ^{1}H, ^{13}C, and ^{19}F NMR spectra of DMSO-d_6,

D_2O, or $CDCl_3$ solutions were recorded on a Varian INOVA 400 spectrometer. The spectrometer operated at 399.6 MHz (^1H), 375.9 MHz (^{19}F), and 100.5 MHz (^{13}C). Chemical shifts in the ^1H NMR and ^{13}C NMR spectra were expressed in parts per million (ppm) vs. TMS as the external standard, and ^{19}F chemical shifts were referenced to $CFCl_3$ as the external standard.

2.2. Preparation of chlorinated products

All solutions were prepared using deionized, carbon filtered water with a chlorine demand of < 10 μmol/L. All reagents were of analytical grade. 5-FU (99%) was purchased from Alfa Aesar. For chlorination experiments, a 15% solution (>15% as Cl) of reagent grade sodium hypochlorite (NaOCl) was obtained from Alfa Aesar. The solution was standardized weekly using an iodometric titration, and the concentration was found to be stable over a period of months. pH was controlled by use of 0.1 M phosphate buffer system in which the pH was adjusted with NaOH.

5-Chloro-5-fluoro-6-hydroxy-5,6-dihydrouracil **(3a)**: Cl_2 was bubbled into a suspension of 5-fluorouracil (**1**; 1.0 g, 7.7 mmol) in 15 mL of water at 25 °C until a clear solution was obtained. The solvent was evaporated to dryness. The resulting white solid was recrystallized from acetone giving 1.2 g (85%) of **3a**. White crystals; m.p. 144 °C. $C_4H_4ClFN_2O_3$ (182.54): calcd. C 26.32, H 2.21, Cl 19.42, F 10.41, N 15.35, O 26.29; found C 26.30, H 2.22, N 15.41. ^1H NMR (400 MHz, DMSO-d_6, 25 °C): δ = 11.1 (s, 1H, N3-H), 8.9 (s, 1H, N1-H), 7.3 (br, 1H, C6-OH), 5.0 (dd, $^3J_{H,H}$ = 5.1 Hz, $^3J_{H,F}$ = 1.9 Hz, 1H, C6-H) ppm. ^{13}C NMR (100 MHz, DMSO-d_6, 25 °C): δ = 163.2 (d, $^3J_{F,C}$ = 27.5 Hz, C4), 151.2 (C2), 97.4 (d, $^2J_{F,C}$ = 254.3 Hz, C5), 77.2 (d, $^3J_{F,C}$ = 26.3 Hz, C6) ppm. ^{19}F NMR (376 MHz, DMSO-d_6, 25 °C): δ = -137.1 (d,

119 $^{3}J_{H,F}$ = 1.9 Hz, C5-F) ppm. MS (ESI-): m/z calcd. for $C_4H_4ClFN_2O_3$ $[M - H]^-$ 181.53; found
120 181.52.
121
122 *2-chloro-2-fluoro-3,3-dihydroxypropanoic acid* **(11)**: Cl_2 was bubbled into a solution of
123 chlorohydrin (**3a**; 300 mg, 1.6 mmol) in 10 mL of water at room temperature, and the course
124 of the reaction was followed by ^{19}F NMR (reaction completed in *ca*. 45 min). The solvent was
125 evaporated to dryness, and 240 mg (95%) of the clean oily product **11** was obtained.
126 $C_3H_4ClFO_4$ (158.51): calcd. C 22.73, H 2.54, Cl 22.37, F 11.99, O 40.37; found C 22.70, H
127 2.57. ^{1}H NMR (400 MHz, DMSO-d_6, 25 °C): δ = 5.0 (d, $^{3}J_{H,F}$ = 14.1 Hz 1H, C3-H) ppm. ^{13}C
128 NMR (100 MHz, DMSO-d_6, 25 °C): δ = 166.2 (d, $^{3}J_{F,C}$ = 27.9 Hz, C1), 104.6 (d, $^{2}J_{F,C}$ = 263.9
129 Hz, C2), 90.4 (d, $^{3}J_{F,C}$ = 20.9 Hz, C3) ppm. ^{19}F NMR (376 MHz, DMSO-d_6, 25 °C): δ = -
130 138.9 (d, $^{3}J_{H,F}$ = 14.1 Hz, C2-F) ppm. MS (ESI-): m/z calcd. for $C_3H_4ClFO_4$ $[M - H]^-$ 157.50;
131 found 157.51.
132
133 *2.3. Daphnia magna Immobilisation Assay*
134
135 The *D. magna* Straus clone MBP996 was purchased as Daphtoxkit F from the MicroBioTests
136 Inc. (Mariakerke, Belgium). *D. magna* neonates were hatched from dormant eggs (ephippia)
137 in Petri dishes containing standard culture media (SCM) and handled according to the
138 supplier instructions. The SCM for *D. magna* was reconstituted in hard water containing
139 $CaCl_2 \times 2H_2O$ (294 mg/L), $MgSO_4 \times 7H_2O$ (123.25 mg/L), $NaHCO_3$ (64.75 mg/L) and KCl
140 (5.75 mg/L) at pH 7.8 ± 0.5. The SCM did not contain any organic compounds. Temperature
141 was maintained at 20 ± 1 °C.
142 The immobilization assay was performed according to the HRN EN ISO 6341:2013 protocol.
143 Neonates were not older than 24 h at the beginning of the test and were transferred in the

glass test vessels containing SCM (control daphnids) or substance 5-FU (**1**), chlorohydrin **3a**, hydrate **11**, or chloral hydrate diluted in SCM at predetermined concentrations (substance exposed daphnids). Transferring procedure was done in order to avoid any hurting of daphnids and causing false positive results. The substance exposure concentrations were prepared in the range 10-1000 mg/L (**1**), 100-1000 mg/L **(3a)**, 85-150 mg/L (**11)** and 350-750 mg/L (chloral hydrate) by diluting the concentrated stock solution in SCM immediately prior to use. The physicochemical properties of the SCM were evaluated to obtain additional information regarding the toxicity test. The temperature, pH, conductivity and oxygen content of the test solutions were assessed at time 0 h and at the end of the exposure time (48 h).

Five *D. magna* neonates (24 h old) were added from Petri dish to each exposure vessels containing 10 mL of SCM (control) or 10 mL solution desired concentration. Daphnids were exposed for 24 and 48 h to the concentrations listed above in four replicates. No food or supplements were added during the exposure period. Neonate immobilization and/or behavioral abnormalities were assessed visually after 24 and 48 h of incubation. The immobilised daphnids were considered those lying on the bottom of the vessels and did not resume swimming within 10 sec after gentle agitation, while swimming in circles or trapping at surface of media were considered as abnormal behavior.

The EC_{50} (i.e., effective concentrations that causes 50% immobilization of the test population) values with the 95% confidence intervals, NOAEC (no observed adverse effect concentration) and LOAEC (lowest observed adverse effect concentration) values were calculated based upon substance concentrations in SCM (Table 1).

2.4. Computational Methods

168 The quantum chemical calculations were performed using the Gaussian09 suite of programs
169 (Frisch et al., 2009). Geometry optimization and frequency calculation were performed at the
170 B3LYP/6-31+G(d) level (Lee et al., 1988; Becke, 1993Improved energetics have been
171 calculated using B2K-PLYP functional (Tarnopolsky et al., 2008). This double-hybrid DFT
172 procedure in combination with 6-311+G(3df,2p) basis set shows the best overall performance
173 for calculating barrier heights for water-catalyzed proton-transfer reactions (Karton et al.,
174 2012). In case of chlorination of amides, the B2K-PLYP model accurately reproduces a high-
175 level composite G3B3 results (Sakic et al., 2014) and has therefore been used throughout the
176 text.

177 Gibbs energies of solvation were determined using the SMD continuum solvation
178 model at the B3LYP/6-31+G(d) level (Marenich et al., 2009). The solvent relative
179 permittivity of $\varepsilon = 78.4$ (water) was used. All other structures, reported throughout the text,
180 include extra water molecules. We found that two explicit water molecules corresponded to
181 „the ideal number of solvent molecules" (Pliego, 2004) for a reliable description of the
182 corresponding potential energy surfaces. . The relative energy of reactants complexed to an
183 optimal number of water is set to zero.

184 In case of all transition state structures the two water molecules were found as an
185 adequate number. Several configurations of explicit water molecules were located in each
186 case, but only the lowest energy transition structures were used for the calculation of the
187 barrier for the corresponding reaction (Sakic et al., 2014).

188 Calculations of NMR chemical shifts and spin couplings were performed at the GIAO-
189 B3LYP/6-311++G(2d,p)//B3LYP/6-31+G(d) and BHandH/6-311++G(2d,p)// B3LYP/6-
190 31+G(d) level, respectively (Gryff-Keller and Szczecinski, 2014).

191

192 **3. Results and Discussion**

193

194 *3.1. The chlorination of 5-fluorouracil*

195

196 The initial site of chlorination of 5-FU is a conflicting issue. In the early report by
197 Miyashita et al. (1982) the chlorination of 5-FU by molecular chlorine (Cl_2) results in the
198 formation of the C5-chlorinated product. whereas the recent study by Li and coworkers (Li et
199 al., 2015) suggests that 5-FU is chlorinated at the C6-position. To resolve the controversy
200 over the reaction regioselectivity, an experimental procedure for chlorination of 5-FU was
201 repeated and product structures were determined by the NMR spectroscopy and mass
202 spectrometry (Table S5).

203

204 *3.1.1. NMR analysis of the reaction mixture*

205

206 The reaction between HOCl and 5-FU (**1**) was followed by ^{1}H and ^{19}F NMR and the
207 obtained spectra confirmed the formation of one product only (Fig 1). In the proton spectrum
208 the resonance signal of C6-H at 7.50 ppm (*d*, $^{3}J_{F,H}$ = 5.5 Hz) disappeared from the aromatic
209 region, and the new doublet showed up at 5.22 ppm (*d*, $^{3}J_{F,H}$ = 2.0 Hz). This upfield shift is
210 consistent with the rehybridization of the C6-carbon atom from sp^2 to sp^3. The multiplicity
211 (doublet) of the signal in ^{1}H NMR spectrum confirms that the C6-hydrogen is coupled to the
212 C5-fluorine in the chlorinated product.

213

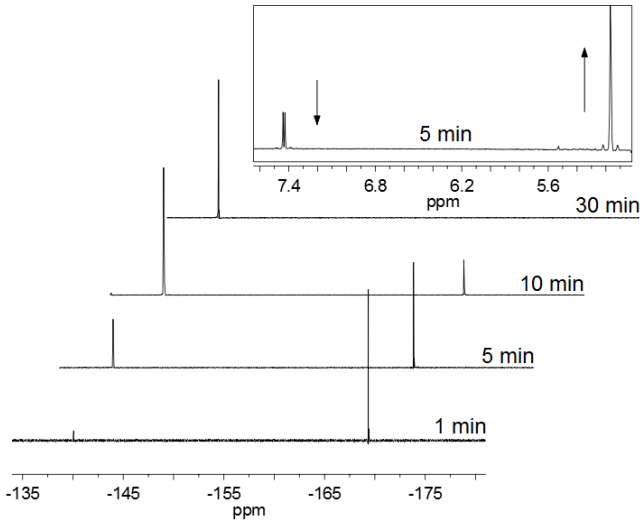

Fig 1. ^{19}F NMR (376 MHz) spectra of the reaction mixture aliquots (5-FU + HOCl in water) taken at several time points. 5-FU concentration 0.05 mol/L, HOCl concentration 0.05 mol/L, pH = 6.7 (phosphate buffer, 0.1 mol/L). The stack-plot of spectra (with an offset included) were recorded over 30 min. The small inset shows ^{1}H NMR (400 MHz) spectrum of the same reaction mixture; arrows point how signals change with time. All spectra were measured at 25 °C (a D_2O filled capillary used).

In the fluorine spectrum (Fig 1), during the course of the reaction, the corresponding doublet of 5-FU ($^{3}J_{F,H}$ = 5.4 Hz, at -169 ppm) was converted to a low-field doublet ($^{3}J_{F,H}$ = 2.0 Hz, at -139 ppm) of the chlorinated product. The small coupling constant observed in ^{1}H and ^{19}F NMR spectra of the product is indicative of a *trans* relation between C6-H and C5-F atoms. In the *cis* isomer the fluorine-hydrogen coupling constant should be much larger ($^{3}J_{F,H}$ > 10 Hz) (Legay, 2014; Robins et al., 1976).

To correctly assign the structure of the chlorinated product, we performed additional NMR analysis. If aqueous solution (or reaction mixture) of the chlorinated product is acidified, a new coupling pattern (*dd*, $^{3}J_{F,H}$ = 2.0 Hz, $^{3}J_{H,H}$ = 5.2 Hz) of a signal at 5.19 ppm appears in the spectrum (Fig S1). The doublet of doublets results from coupling of C6-H to both C5-F and N1-H. It was shown earlier that splitting of C6-H with amide proton in uracil

could be observed when exchange of N1-H was sufficiently slow (e.g. inhibited by the addition of acid) (Hurd and Reid, 1977; Kokko and Mandell, 1962). It is also possible to detect a coupling of C6-H with C6-OH if the chlorinated product is dissolved in d_6-DMSO, and small amount of HCl is added. The corresponding coupling constant ($^3J_{H,H}$) of 4.9 Hz is very similar to that observed for interaction between C6-H and N1-H ($^3J_{H,H}$ = 5.1 Hz), which results in the superposition of two doublets. The appearance of triplet of doublets at 4.97 ppm (Fig S2) is due to the additional coupling constant of 1.9 Hz for splitting between C6-H and C5-F.

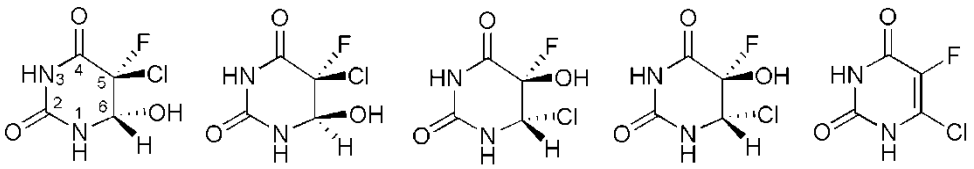

Chart 1. Proposed structures of the initial product in the reaction between HOCl and 5-FU, which are considered in recently reported studies or in this work.

All this points to the chlorohydrin structure **3a** in which the C5-position is chlorinated and the C6-position is hydroxylated (Chart 1). The *cis* isomer **3b** may be rule out as a product on the basis of ^{19}F-^{1}H coupling constants (see above), and because of the unfavorable reaction pathway calculated for its formation (see calculations below). Structural properties of isomers **4a** and **4b** are also not in accordance with the measured NMR data. Finally, in case of C6-chlorinated fluorouracil (**5**), *i.e.* the product which was suggested by Li et al. (2015), the fluorine signal should be observed as a singlet in the coupled ^{19}F NMR spectrum.

Key data from the experimental NMR study have been reproduced by DFT GIAO-NMR calculations (Gryff-Keller and Szczecinski, 2014). The ^{13}C and ^{19}F NMR chemical shifts and corresponding coupling constants were calculated for the parent 5-FU, for

chlorohydrins **3a** – **4b** as plausible product structures (Chart 1), and for the C6-chloro-5-fluorouracil (**5**) proposed earlier (see Table S1) (Li et al., 2015). ^{19}F NMR chemical shifts were found as sensitive tool to assign the correct structure of the chlorohydrin product. By comparing experimental and calculated chemical shifts it is possible to discriminate between C5- and C6-chlorinated chlorohydrin structures **3** and **4**, respectively. In chlorohydrins **3a** and **3b**, the calculated chemical shift for C5-F is -135.3 and -134.7 ppm, which is very close to experimental value of -137 ppm. In chlorohydrins **4a** and **4b**, however, the corresponding peaks are shifted by ~20 ppm downfield. In addition, the experimental value for one-bond fluorine-carbon coupling is 255.9 Hz, and this value can be reproduced only for C5-chlorinated structures **3a** ($^{1}J_{F,C}$ = 256.3 Hz) and **3b** ($^{1}J_{F,C}$ = 249.2 Hz). Therefore, the C6-carbon atom can be rejected as a possible site of chlorination of 5-fluorouracil.

As well, it is straightforward to compare experimental and calculated ^{19}F-^{1}H couplings to interpret the stereochemistry in C5-chlorinated chlorohydrins. The experimental value of 2.0 Hz for ^{19}F-^{1}H splitting can be correctly reproduced only if *trans*-chlorohydrin **3a** is taken into account (calculated $^{3}J_{F,H}$ = 2.9 Hz). In the presumed *cis*-isomer **3b** this value amounts to 7.8 Hz.

^{13}C NMR calculated chemical shifts are not informative (Table S1), as values for all chlorohydrins are scattered around experimental data, while calculated two-bond fluorine-carbon couplings do not offer reliable tool to discriminate between the proposed structures in Chart 1. In conclusion, only chlorohydrin structure **3a** fits well to calculated and experimental NMR data.

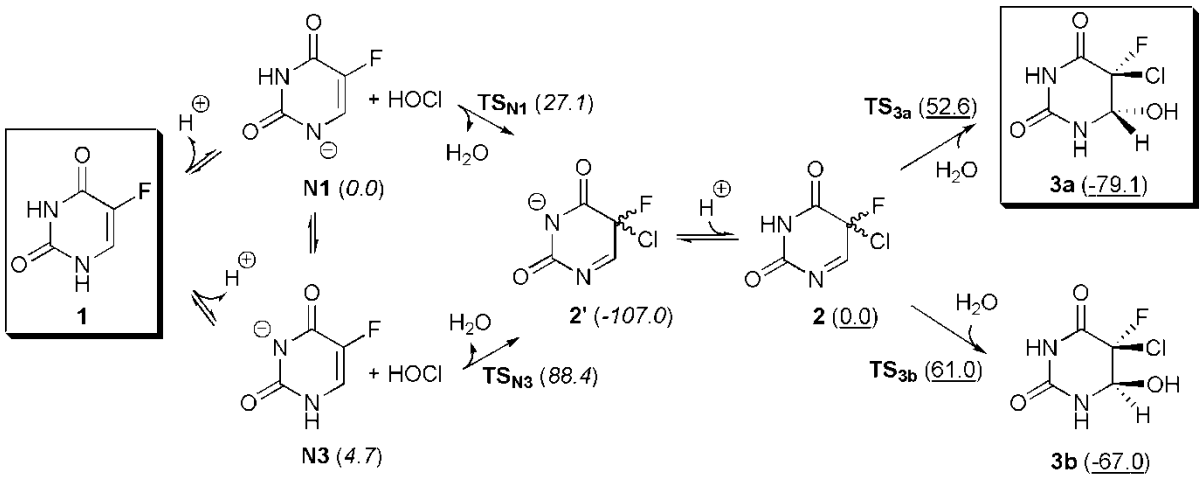

Scheme 1. The reaction mechanism for chlorination of 5-fluorouracil anions **N1** and **N3**. Relative Gibbs free energies (ΔG_{298} in kJ/mol, in parentheses) calculated at the B2K-PLYP/6-311+G(3df,2p)//B3LYP/6-31+G(d) level are given in italics (**N1** is set to zero for the anionic pathway) and in underlined format (**2** is set to zero for the neutral pathway). For clarity, the two explicit water molecules included in calculations are not presented.

3.1.2. Quantum chemical study of the chlorination of 5-FU

Different mechanisms, underlying the reaction between 5-FU and HOCl, were probed by the use of computational models. The epoxidation of the C5-C6 double bond in 5-FU, the one-step addition of HOCl on C5-C6 double bond, and C5- and C6-hydroxylation processes were considered, but calculated barriers for these alternative processes were prohibitively high, and therefore all are deposited in Supporting Information (Scheme S1).

According to quantum-chemical calculations the most favorable process involves HOCl and 5-FU anion as reactants (Scheme 1). The molecular form of 5-FU is a predominant species in a neutral aqueous solution (pK_a of 5-FU is 7.93) (Diaz-Gavilan et al., 2006), but the anion form is expected to be much more reactive. It was shown that bromination of uracil

296 anion is several order of magnitude faster than the corresponding reaction with the molecular
297 form of uracil (Tee and Berks, 1980).
298 The 5-FU anion exists as an equilibrium mixture of two monoanions, *i.e*. N3- and N1-
299 species (Scheme 1) (Wierzchowski et al., 1965). They are present in aqueous solution in the
300 ratio of 2 : 3, respectively (Abdrakhimova et al., 2014), and the observed pK_a for 5-
301 fluorouracil is a composite of the overlapping ionizations of the N1 and N3 positions.
302 Nucleophilic reactivities of these two anions, however, could be quite different. It has been
303 suggested that the imide anion is much better solvated in water and is, therefore, significantly
304 less reactive than the amide anion (Breugst et al., 2012).
305 Our computational results support these experimental findings. All calculations were
306 performed at the B2K-PLYP/6-311+G(3df,2p)//B3LYP/6-31+G(d) level of theory, and all
307 stationary points located at the potential energy surface include two explicit water molecules
308 (not presented in Scheme 1). We located two transition state structures **TS$_{N1}$** and **TS$_{N3}$**
309 (Scheme 1 and Fig S3) for the C5-chlorination of anions **N1** and **N3**, respectively. The
310 corresponding barriers are 27.1 and 88.4 kJ/mol, respectively, which supports a claim that
311 amide anion **N1** is more nucleophilic towards Cl^+ cation (values are given in Scheme 1). In
312 both reactions the imine intermediate **2'** is formed, which is 107.0 kJ/mol more stable than the
313 starting reactants, *i.e*. the separated reactants **N1** and HOCl. The results from our calculations
314 performed at different level of theory are presented in Table S2.
315 The involvement of the imine was confirmed earlier in the course of the bromination
316 of uracil (Tee and Berks, 1980; Henderson et al., 2001), and here we suggest it as an
317 intermediate in the course of chlorination of 5-fluorouracil. In water the imine **2** undergoes
318 the addition of water which can result in either *trans*- or *cis*-chlorohydrin products (**3a** or **3b**).
319 Our computational results suggest that the *anti*-addition (i.e. water approaches the N1-C6
320 double bond at the side opposite to the C5-Cl bond) is a faster process ($\Delta G^{\ddagger}_{anti}$ = 52.6 kJ/mol)

than the *syn*-attack of water ($\Delta G^{\ddagger}_{syn}$ = 61.0 kJ/mol). The respective transition state structures **TS$_{3a}$** (for reaction **2** → **3a**) and **TS$_{3b}$** (for reaction **2** → **3b**) are presented in Fig S4. The *anti*-addition of water to imine **2** results in *trans*-chlorohydrin **3a** which is 12.1 kJ/mol more stable than the *cis*-isomer **3b** (Scheme 1). Therefore, the formation of **3a** is both thermodynamically and kinetically favored. This is in agreement with experimental findings that chlorination of 5-FU results in only one product, and fits to the measured NMR ^{19}F-^{1}H coupling data (see above) which indicate *trans*-stereochemistry of the chlorohydrin formed.

*3.2. The chlorination of trans-chlorohydrin **3a***

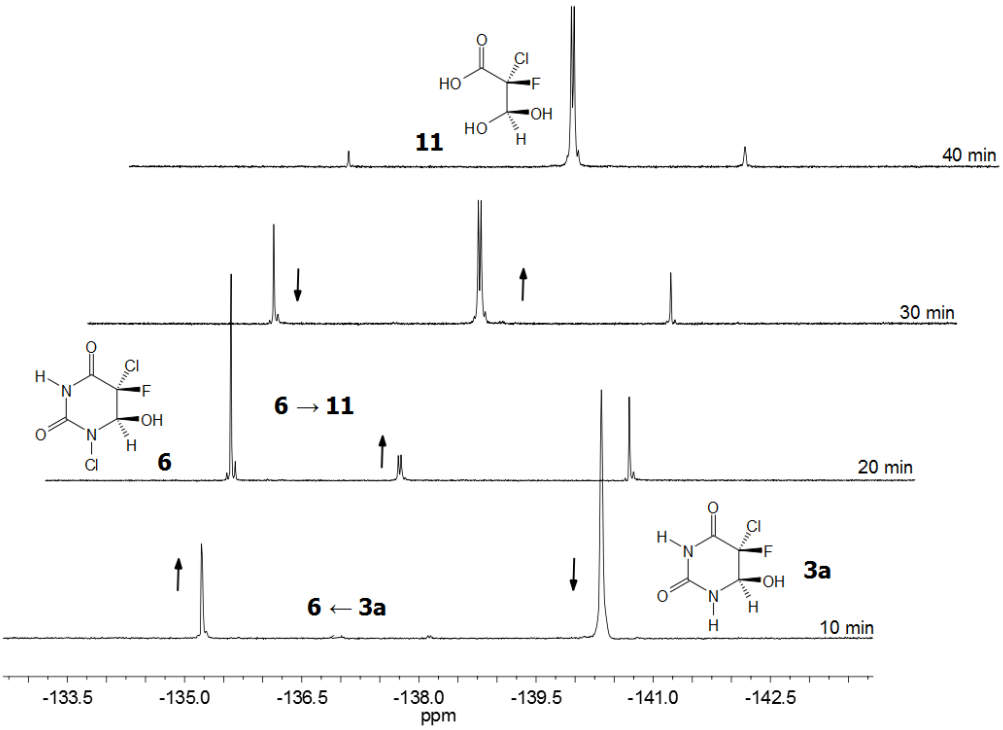

Fig 2. ^{19}F NMR (376 MHz) spectra of the reaction mixture aliquots (**3a** + HOCl in water) taken at several time points. Chlorohydrin **3a** concentration 0.05 mol/L, HOCl concentration 0.1 mol/L, pH =6.7 (phosphate buffer, 0.1 mol/L). The stack-plot of spectra (with an offset included) were recorded over 40 min; arrows point how signals change with time. All spectra were measured at 25 °C (a D_2O filled capillary used).

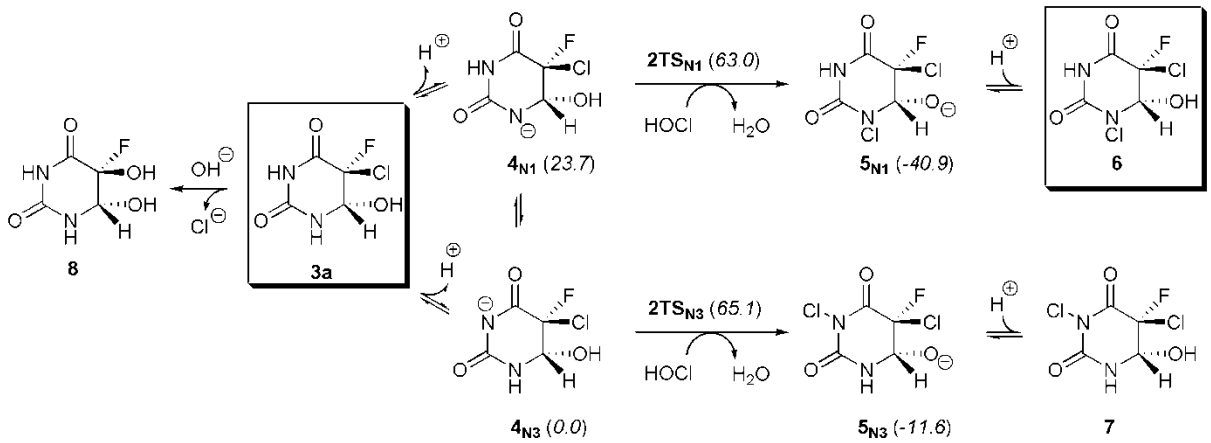

Scheme 2. The reaction mechanism for chlorination of the chlorohydrin **3a**. Relative Gibbs free energies (ΔG_{298} in kJ/mol, in parentheses) calculated at the B2K-PLYP/6-311+G(3df,2p)//B3LYP/6-31+G(d) level are given in italics (**4**$_{N3}$ is set to zero for anionic pathway only). For clarity, the two explicit water molecules included in calculations are not presented.

In basic aqueous medium (pH = 10-11) the chlorohydrin **3a** is easily converted to glycol **8** (Scheme 2). Upon addition of NaOH to aqueous solution of **3a**, only one signal (at -122.03 ppm) was observed in the ^{19}F NMR spectra, while the corresponding ^{1}H and ^{13}C NMR data (Fig S8) were consistent with the structure of the glycol **8** (Scheme 2). The glycol **8** is, however, out of the scope of the present study and has not been tested for its ecotoxicity.

In neutral or slightly acidic medium, the chlorohydrin **3a** undergoes N-chlorination induced by HOCl, which may result in either N1- or N3-chlorinated product (**6** and **7** in Scheme 2). In the ^{19}F NMR spectrum of the reaction mixture (Fig 2) a new signal appeared at -135.25 ppm, which suggested the formation of one product only (the same reaction occurs and the same product was detected when the parent 5-FU is subjected to a prolonged chlorination reaction time). In order to isolate and identify the unstable N-chlorinated intermediate, the reaction mixture was sampled and treated by chloroform. In this solvent the

chlorohydrin **3a** is insoluble, but the N-chlorinated product is slightly soluble. In the ^{1}H NMR of the extracted N-chlorinated product only one NH signal is observed at 8.10 ppm which corresponds to imide N3-proton (Fig S9). In addition, a new doublet ($^{3}J_{F,H}$ = 2.0 Hz) appears in the spectrum at 5.36 ppm. Contrary to the chlorohydrin **3a**, no coupling between C6-H and N1-H protons was observed when HCl is added to aqueous solution (see above). All this indicates that N1-position is chlorinated, i.e. that the reaction between HOCl and chlorohydrin **3a** results in chloroamide **6** (Scheme 2).

The regioselective chlorination of amide N1-position (vs. imide N3-position) can be rationalized by computational results. Both N1- and N3-anionic forms of chlorohydrin **3a** have been considered as a reactive species in the reaction with HOCl. The corresponding energy barriers for the addition of Cl^{+} ion to N1- and N3-position are very similar (i.e. the corresponding transition states **2TS$_{N1}$** and **2TS$_{N3}$** are close in energy, Scheme 2 and Fig S5), and therefore the kinetic control cannot be accounted for the observed regioselectivity. However, the product of N1-chlorination (**5$_{N1}$**) was calculated more stable (ΔG_{298} = 29.3 kJ/mol) than the corresponding product of N3-chlorination (**5$_{N3}$**), which strongly suggested that regioselectivity of N-chlorination in chlorohydrin **3a** was thermodynamically driven.

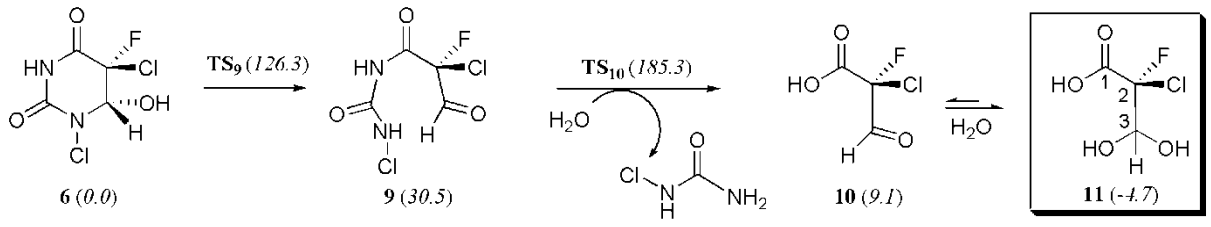

Scheme 3. The reaction mechanism for the intramolecular proton transfer and ring opening in **6** (set to zero), and subsequent hydrolysis of **9** resulting in the final product **11** (exists in equilibrium with the aldehyde form **10**).

In aqueous medium the chloroamide intermediate **6** may be converted to the final product **11** (Scheme 3). It was demonstrated earlier that *N*-chlorination of the chlorohydrin intermediate promoted the pyrimidine ring opening in the uracil system (Young and Uden, 1994). It was also shown that water was essential for that reaction to occur.

The chlorination of N1-position induced an intramolecular proton transfer in **6**. The C6-OH proton is shifted to the N1-Cl group, which makes N1-C6 bond very labile and prone to the cleavage process **6** → **9**. The amide bond in the short-lived intermediate **9** is hydrolyzed resulting in the elimination of the chlorinated urea. In this process the aldehyde **10** is produced, which is easily converted to the final product **11**. None of the two intermediates, **9** and **10**, were detected by ^{1}H or ^{19}F NMR during the course of the reaction.

These two reaction steps, **6** → **9** and **9** → **10**, were investigated by means of DFT calculations which support the mechanism proposed in Scheme 3. The first transition state **TS$_9$** corresponds to the structure in which the intramolecular proton transfer occurs concurrently with the pyrimidine ring opening (Fig S6). The calculated barrier for this process amounts to 126.3 kJ/mol. It is interesting to note that the calculated energy barrier for the analogous proton transfer (C6-O to N1) in the chlorohydrin **3a** is much higher ($\Delta G^{\ddagger}$ = 149.1 kJ/mol). Therefore, the chlorohydrin intermediate **3a** is resistant to the ring opening process, unless the N1-position is chlorinated. The second transition state **TS$_{10}$**, which represents the rate determining step, corresponds to the hydrolysis of the amide (see Fig S7 for details). This is a two-step consecutive process which follows the general mechanism for amide hydrolysis reported earlier (Pliego, 2004; Bachrach and Dzierlenga, 2011). The calculated energy barrier for the hydrolysis step is somewhat high, but is lowered significantly when acid or base catalysis is included. Due to simplicity, only the neutral pathway was considered in the calculations (Scheme 3).

In short, the chlorohydrin product **3a** can be converted to hydrate **11**, only after the chlorination at the N1-position. This is exactly what was recorded by our NMR experiment, in which all three species **3a**, **6**, and **11** were observed simultaneously (Fig 2). This reveals that the reaction channel **3a** → **6** → **11** is indeed operative.

The similar reaction sequence was established in case of uracil chlorination, in which the trichloroacetaldehyde (Cl_3CCHO), or chloral hydrate ($Cl_3CC(OH)_2$), was detected as the final product (Young and Uden, 1994). Chloral hydrate is structurally and electronically related to hydrate **11**, which exists in equilibrium with its aldehyde form **10** (Scheme 3). In general, aldehydes are more stable than the hydrate counterparts, but electron-withdrawing groups may shift the equilibrium toward the latters (Smith, 2013). In case of the trichloroacetaldehyde, the three chlorine atoms withdraw electron density from the partially positive carbon atom, which destabilizes the carbonyl bond, whereas the aldehyde **10** is destabilized by the similar electron-withdrawing effect of carboxyl group, fluorine and chlorine atoms. Therefore, in both cases hydrates are predominate forms in the corresponding equilibria. For that reason the ecotoxicity properties of the two hydrates were compared in *Daphnia magna* immobilization assays (see below).

*3.3. Ecotoxicity results for **1**, **3a**, **11**, and chloral hydrate*

A number of data exist on the toxic effects of the parent 5-FU (**1**) on *D. magna* immobilisation, with EC_{50} values ranging from 15 mg/L to 319 mg/L. Higher toxicity of 5-FU (15 – 36 mg/L) was reported in earlier studies (Zounkova et al., 2010; Cleuvers, 2002; Straub, 2010; Parrella et al., 2014; Zounkova et al., 2007), while the most recent result of EC_{50} (319 mg/L) was an order of magnitude higher, suggesting that 5-FU is only slightly toxic to *D. magna* (Harris, 2015). In the latter study the large variation of EC_{50} values was discussed

thoroughly, including details on protocols, growth media, solvents, etc. In our study we followed the protocol according to the HRN EN ISO 6341:2013, which is comparable to the procedure reported by Harris (Harris, 2015). Our result (EC_{50} = 285.8 mg/L) approaches the most recent result (319 mg/L), and shows that 5-FU induces only negligible toxicity to *D. magna* (Table 1). In addition, this is supported by an environmental risk assessment in which authors claimed that EC_{50} for 5-FU must be over 100 mg/L (Załęska-Radziwiłł et al., 2011).

Table 1

Ecotoxicity of 5-FU (**1**), chlorohydrin **3a**, the mixture of **1** and **3a**, hydrate **11**, and chloral hydrate (all values in mg/L).

Substance	NOAEC	LOAEC	EC_{50}(24h)	EC_{50}(48h)
5-FU (**1**)	5	10	-	285.8
Chlorohydrin **3a**	50	100	-	425.5
1 + **3a** (1 : 1)	65 (48 h)	85 (48 h)	-	116.7
Hydrate **11**	100 (24h)	125 (24 h)	138	122.0
	50 (48 h)	85 (48 h)		
Chloral hydrate	350	450	586	537.0

The same test with *D. magna* immobilization was carried out to assess the ecotoxicological effects of the chlorohydrin product **3a**, which is the first chlorinated derivative of the 5-FU. Obtained data demonstrated that microcrustacean were more sensitive to the parent 5-FU than to its chlorinated product **3a** with an EC_{50} (48 h) of 425.5 mg/L. It appears that chlorination of 5-FU results in the product which has much lower (eco)toxicity. According to the EU-Directive 93/67/ EEC (EC, 1996), the chlorohydrin product **3a** may be classified as nontoxic.

In addition, we performed ecotoxicity test for the mixture of 5-FU and chlorohydrin **3a** (1 : 1) and obtained an EC_{50} (48 h) of 116.7 mg/L. Therefore, the mixture of 5-FU and its chlorinated product is more toxic to *D. magna* than any individual component, which suggests a possible interaction between the two substances.

449 The prolonged chlorination of 5-FU gives rise to the hydrate **11** in which the pyrimidine ring
450 opening occurred. This chlorinated byproduct was found more toxic to *D. magna* than either
451 of the two precursors (5-FU and chlorohydrin **3a**). The EC_{50} data at 24 h and 48 h were 138
452 mg/l and 122 mg/l, respectively. We compared these results to the EC_{50} value obtained for
453 chloral hydrate, a well known sedative and hypnotic drug, which is structurally related to
454 hydrate **11**. The measured EC_{50} values for 24 h and 48 h were 586 mg/L and 537 mg/l,
455 respectively, which is in a good agreement with reported data for chloral hydrate ranging
456 between 500 – 630 mg/L (Bringmann and Kuhn, 1982). Therefore, among the four tested
457 single substances, the hydrate **11** is evidently the most harmful compound in terms of *D.*
458 *magna* immobilization, which is used hereby as a toxicity assessment criterion.
459 Our results reveal a composite effect of chlorination on the ecotoxicity profile of 5-FU
460 (**1**) and its chlorinated metabolites. The adverse effect of chlorinated species depends on the
461 extent of chlorination, with the first chlorination product (chlorohydrin **3a**) being less toxic
462 than the parent, while the toxicity enhances by a prolonged chlorination (hydrate **11**). The
463 final chlorination product exists in a fast equilibrium between its aldehyde (**10**) and hydrate
464 (**11**) form (see Scheme 3), and therefore is not easy to resolve which species is more relevant
465 for the observed toxicity.
466
467 **4. Conclusions**
468
469 A detailed mechanism underlying the chlorination of 5-fluorouracil was explored by
470 use of NMR analysis and quantum chemical calculations. In neutral aqueous solution the
471 reactive species are *N*-anionic form of 5-FU and HOCl as a chlorinating agent. Both ^{1}H and
472 ^{19}F NMR spectra of the reaction mixture confirm the formation of only one product, which

corresponds to a chlorohydrin structure **3a**. With the finding that the chlorination occurs at the C5-position, the old controversy on the site of the 5-FU chlorination has come to a closure.

The chlorohydrin itself may undergo chlorination at the N1-position, which resulted in the formation of the hydrate **11**. Therefore, the chlorination of the parent 5-FU produces at least two stable transformation species – chlorohydrin **3a** as the primary product, and the hydrate **11**, which emerged if the chlorination procedure with HOCl was prolonged.

To complete the whole reaction profile quantum chemical calculations, at the B2K-PLYP//B3LYP level were employed to describe the corresponding energy surface. We found this DFT model sufficient to support and interpret experimental data.

The two isolated chlorinated product are of relevance for the chemical fate of 5-FU under chlorinating conditions. For that reason, their ecotoxicological profile was assessed by *Daphnia magna* immobilization test. The first chlorinated product chlorohydrin **3a** was less toxic than the parent 5-FU, suggesting the beneficial effect of chlorination. The second chlorinated product hydrate **11**, however, exhibited increased ecotoxicity. Therefore, the existence (and related toxicity) of chlorinated products of 5-FU in treated wastewaters may be a function of contact time with a chlorinating agent, which is an interesting feature from the environmental point of view.

Conflicts of interest

The authors declare no conflict of interest.

Acknowledgments

We thank the Computing Centre SRCE of the University of Zagreb for allocating computer time on the Isabella cluster where a part of the calculations was performed.

498

499 **References**

500

501 Abdrakhimova G. S., Ovchinnikov M. Y., Lobov A. N., Spirikhin L. V., Ivanov S. P. and
502 Khursan S. L., 2014, 5-Fluorouracil solutions: NMR study of acid–base equilibrium in
503 water and DMSO. J. Phys. Org. Chem., 27, 876-883. DOI: 10.1002/poc.3350.
504 Acero J. L., Benitez F. J., Real F. J. and Roldan G., 2010, Kinetics of aqueous chlorination of
505 some pharmaceuticals and their elimination from water matrices. Water Res., 44, 4158-
506 4170. DOI: 10.1016/j.watres.2010.05.012.
507 Bachrach S. M. and Dzierlenga M. W., 2011, Microsolvation of uracil and its conjugate
508 bases: a DFT study of the role of solvation on acidity. J. Phys. Chem. A, 115, 5674-5683.
509 DOI: 10.1021/jp202548h.
510 Becke A. D., 1993, Density-functional thermochemistry. III. The ole of exact exchange. J.
511 Chem. Phys. 98, 5648-5652. DOI: 10.1063/1.464913.
512 Breugst M., Bautista F. C. and Mayr H., 2012, Nucleophilic reactivities of the anions of
513 nucleobasees and their subunits. Chem. Eur. J., 18, 127-137. DOI:
514 10.1002/chem.201102411.
515 Bringmann G. and Kuhn R., 1982, Results of toxic action of water pollutants on *Daphnia*
516 *magna* straus tested by an improved standardized procedure. Wasser-Abwasser-Forsch, 15,
517 1-6.
518 Cleuvers M., 2002, Aquatische ökotoxikologie ausgewahlter arzneimittel. Z. Umweltchem.
519 Okotox., 14, 85-89. DOI: org110.1065/uwsf2002.04.025.
520 Deborde M. and Gunten U., 2008, Reactions of chlorine with inorganic and organic
521 compounds during water treatment-Kinetics and mechanisms: a critical review. Water.
522 Res., 42, 13-51. DOI: 10.1016/j.watres.2007.07.02.

523 Diaz-Gavilan M., Gomez-Vidal J. A., Entrena A., Gallo M. A., Espinosa A., and Campos J.
524 M., 2006, Study of the factors that control the ratio of the products between 5-fluorouracil,
525 uracil, and tetrahydrobenzoxazepine O,O-acetals bearing electron-withdrawing groups on
526 the nitrogen atom. J. Org. Chem., 71, 1043-1054. DOI: 10.1021/jo052167m.
527 EC, 1996. Technical guidance document in support of commission directive 93/67/EEC on
528 risk assessment for existing substances. Part II; Environmental risk assessment.
529 Luxembourg, Office for Official Publications of the European Communities.
530 Frisch, M.J., Trucks, G.W., Schlegel, H.B., Scuseria, G.E., Robb, M.A., Cheeseman, J.R.,
531 Scalmani, G., Barone, V., Mennucci, B., Petersson, G.A., Nakatsuji, H., Caricato, M., Li,
532 X., Hratchian, H.P., Izmaylov, A.F., Bloino, J., Zheng, G., Sonnenberg, J.L., Hada, E.M.,
533 Toyota, K., Fukuda, R., Hasegawa, J., Ishida, M., Nakajima, T., Honda, Y., Kitao, O.,
534 Nakai, H., Vreven, T., Montgomery, J.A., Peralta, J.E., Ogliaro, F., Bearpark, M., Heyd,
535 J.J., Brothers, E., Kudin, K.N., Staroverov, V.N., Kobayashi, R., Normand, J.,
536 Raghavachari, K., Rendell, A., Burant, J.C., Iyengar, S.S., Thomas, J., Cossi, M., Rega, N.,
537 Millam, J.M., Klene, M., Knox, J.E., Cross, J.B., Bakken, V., Adamo, C., Jaramillo, J.,
538 Gomperts, R., Stratmann, R.E., Yazyev, O., Austin, A.J., Cammi, R., Pomelli, C.,
539 Ochterski, J.W., Martin, R.L., Morokuma, K., Zakrzewski, V.G., Voth, G.A., Salvador, P.,
540 Dannenberg, J.J., Dapprich, S., Daniels, A.D., Farkas, O., Foresman, J.B., Ortiz, J.V.,
541 Cioslowski, J., Fox, D.J., 2009. Gaussian 09, Revision D.01. Gaussian Inc, Wallingford
542 CT.
543 Gryff-Keller A. and Szczecinski P., 2014, A successful DFT calculation of carbon-13 NMR
544 chemical shifts and carbon–fluorine spin–spin coupling constants in (η6-
545 fluoroarene)tricarbonylchromium complexes. RSC Adv., 4, 27290-27296. DOI:
546 10.1039/c4ra01249f.

547 Harris G., 2015, A Comparison of aquatic species responses to anticancer drug exposure.
548 PhD Thesis, Brunel University, London, UK.
549 Henderson J. P., Byun J., Mueller D. M. and Heinecke J. W., 2001, The eosinophil
550 peroxidase-hydrogen peroxide-bromide system of human eosinophils generates 5-
551 bromouracil, a mutagenic thymine analogue. Biochemistry, 40, 2052-2059. DOI:
552 10.1021/bi002015f.
553 Hurd R. E. and Reid B. R., 1977, NMR spectroscopy of the ring nitrogen protons of uracil
554 and substituted uracils; relevance to A Ψ base pairing in the solution structure of tranfer
555 RNA. Nucl. Acid Res., 4, 2747-2756. DOI: 10.1093/nar/4.8.2747
556 Jordan V. C., 2016, A retrospective: On clinical studies with 5-fluorouracil. Cancer. Res., 76,
557 767-768. DOI: 10.1158/0008-5472.CAN-16-0150.
558 Karton A., O'Reilly R. J. and Radom L., 2012, Assessment of theoretical procedures for
559 calculating barrier heights for a diverse set of water-catalyzed proton-transfer reactions. J.
560 Phys. Chem. A, 116, 4211-4221. DOI: 10.1021/jp301499y.
561 Kokko J. P. and Mandell L., 1962, An N.m.r. Investigation of proton mobility in substituted
562 uracils. J. Am. Chem. Soc., 84, 1042-1047. DOI: 10.1021/ja00865a035.
563 Kosjek T. and Heath E., 2011, Occurrence, fate and determination of cytostatic
564 pharmaceuticals in the environment. Trends Anal. Chem., 30, 1065-1087. DOI:
565 10.1016/j.trac.2011.04.007.
566 Kosjek T., Perko S., Žigon D. and Heath E., 2013, Fluorouracil in the environment: Analysis,
567 occurrence, degradation and transformation. J. Chromatogr. A, 1290, 62-72. DOI:
568 10.1016/j.chroma.2013.03.046.
569 Lee C., Yang W. and Parr R. G., 1988, Development of the Colle-Salvetti correlation-energy
570 formula into a functional of the electron density. Phys. Rev. B Condens. Matter, 37, 785-
571 789. DOI: 10.1103/PhysRevB.37.785.

572 Legay R. J., 2014, Hydrolytic pathway of 5-fluorouracil in aqueous solutions for clinical use.
573 Pharm. Biomed. Anal., 98, 446-462. DOI: 10.1016/j.jpba.2014.06.015.
574 Li W., Tanumihardja J., Masuyama T. and Korshin G., 2015, Examination of the kinetics of
575 degradation of the antineoplastic drug 5-fluorouracil by chlorine and bromine. J. Haz.
576 Mat., 282, 125-132. DOI: 10.1016/j.jhazmat.2014.05.090
577 Mahnik S. N., Rizovski B., Furhacker M. and Mader R. M., 2004, Determination of 5-
578 fluorouracil in hospital effluents. Anal. Bioanal. Chem., 380, 31-35. DOI: 10.1007/s00216-
579 004-2727-6.
580 Mahnik S. N., Lenz K., Weissenbacher N., Mader R. M. and Furhacker M., 2007, Fate of 5-
581 fluorouracil, doxorubicin, epirubicin, and daunorubicin in hospital wastewater and their
582 elimination by activated sludge and treatment in a membrane-bioreactor system.
583 Chemosphere, 66, 30-37. DOI: 10.1016/j.chemosphere.2006.05.051.
584 Marenich V., Cramer C. J. and Truhlar D. G., 2009, Universal solvation model based on
585 solute electron density and on a continuum model of the solvent defined by the bulk
586 dielectric constant and atomic surface tensions. J. Phys. Chem. B, 113, 6378-6396. DOI:
587 10.1021/jp810292n.
588 Miyashita O., Kasahara T., Matsumura K., Shimadzu H., Takamoto M. and Hashimoto N.,
589 1982, Studies on fluorinated pyrimidines. IV. Stereochemistry of 6-alkoxyl-5-fluoro-5,6-
590 dihidrouracils and 5-alkoxycarbonyl-5-fluoro-6-substituted-5,6-dihidroracils. Chem.
591 Pharm. Bull., 30, 2333-2341. DOI: 10.1248/cpb.30.2333.
592 Parrella A., Lavorgna M., Criscuolo E., Russo C., Fiumano V. and Isidori M., 2014, Acute
593 and chronic toxicity of six anticancer drugs on rotifers and crustaceans. Chemosphere, 115,
594 59-66. DOI: 10.1016/j.chemosphere.2014.01.013.

595 Pliego Jr. J. R., 2004, Basic hydrolysis of formamide in aqueous solution: A reliable
596 theoretical calculation of the activation free energy using the cluster-continuum model.
597 Chem. Phys., 306, 273-280. DOI: 10.1016/j.chemphys.2004.07.041.
598 Robins M. J., MacCoss M., Naik S. R. and Ramani G., 1976, Nucleic acid related compounds.
599 21. Direct fluorination of uracil and cytosine bases and nucleosides using trifluoromethyl
600 hypofluorite. Mechanism, stereochemistry, and synthetic applications. J. Am. Chem. Soc.,
601 98, 7381-7389. DOI: 10.1021/ja00439a046.
602 Sakic D., Sonjic P., Tandaric T. and Vrcek V., 2014, Chlorination of N-methylacetamide and
603 amide-containing pharmaceuticals. Quantum-chemical study of the reaction mechanism. J.
604 Phys. Chem. A, 118, 2367-2376. DOI: 10.1021/jp5012846.
605 Smith M. B., March's Advanced organic chemistry: Reactions, mechanisms, and structure.
606 Wiley, New Jersey, 2013, p 1262.
607 Straub J. O., 2010, Combined environmental risk assessment for 5-fluorouracil and
608 capecitabine in Europe. Integrated environmental assessment and management. Integr.
609 Environ. Assess Manag., 6, 540-566. DOI: 10.1897/IEAM_2009-073.1.
610 Tarnopolsky A., Karton A., Sertchook R., Vuzman D. and Martin J. M. L., 2008, Double-
611 hybrid functionals for thermochemical kinetics. J. Phys. Chem. A, 112, 3-8. DOI:
612 10.1021/jp710179r
613 Tee O. S. and Berks C. G., 1980, Mechanisms of bromination of uracil derivatives. 5.
614 Reaction of uracil and 5-bromouracil via their anions in weakly acidic aqueous solution. J.
615 Org. Chem., 45, 830-835. DOI: 10.1021/jo01293a014.
616 USEPA, 2004. Guidelines for water reuse. Publication EPA625/R-04/951 108. U.S.
617 Environmental Protection Agency, Washington, DC.
618

619 Wierzchowski K. L., Litońska E. and Shugar D., 1965, Infrared and ultraviolet studies on the
620 tautomeric equilibria in aqueous medium between monoanionic species of uracil, thymine,
621 5-fluorouracil, and other 2,4-diketopyrimidines. J. Am. Chem. Soc., 87, 4621-4629. DOI:
622 10.1021/ja00948a039.
623 Winterbourn C. C., Kettle A.J. and Hampton M. B., 2016, Reactive oxygen species and
624 neutrophil function. Ann. Rev. Biochem., 85, 765-792. DOI: 10.1146/annurev-biochem-
625 060815-014442.
626 Young M. S. and Uden P.C., 1994, Byproducts of the aqueous chlorination of purines and
627 pyrimidines. Environ. Sci. Technol., 28, 1755-1127. DOI: 10.1016/S0006-3495(03)74548-
628 2.
629 Załęska-Radziwiłł M., Łebkowska M., Katarzyna A. and Agnieszka Z., 2011, Environmental
630 risk assessment of selected pharmaceuticals present in surface water in relation to animals.
631 Arch. Environ. Pro., 37, 31-42.
632 Zounkova R., Kovalova L., Blaha L. and Dott W., 2010, Ecotoxicity and genotoxicity
633 assessment of cytotoxic antineoplastic drugs and their metabolites. Chemosphere, 81, 253-
634 260. DOI: 10.1016/j.chemosphere.2010.06.029.
635 Zounková R., Odráska P., Dolezalová L., Hilscherová K., Marsálek B. and Bláha L., 2007,
636 Ecotoxicity and genotoxicity assessment of cytostatic pharmaceuticals. Environ. Toxicol.
637 Chem., 26, 2208-2214. DOI: 10.1897/07-137R.1.
638

639